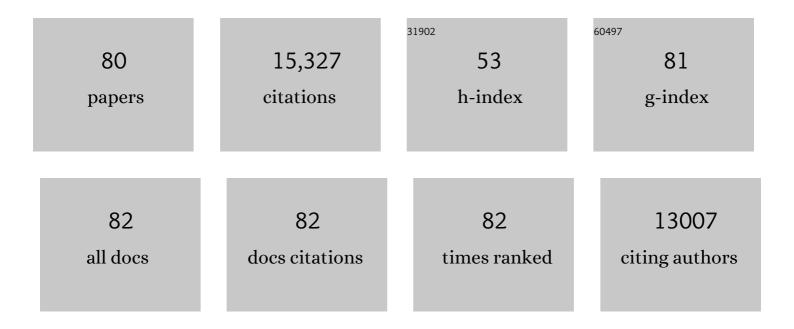
List of Publications by Year in descending order

Source: https://exaly.com/author-pdf/8443798/publications.pdf Version: 2024-02-01



#	Article	IF	CITATIONS
1	Ultrathin 2D/2D WO3/g-C3N4 step-scheme H2-production photocatalyst. Applied Catalysis B: Environmental, 2019, 243, 556-565.	10.8	1,895
2	g <sub>3</sub> N <sub>4</sub> â€Based Heterostructured Photocatalysts. Advanced Energy Materials, 2018, 8, 1701503.	10.2	1,870
3	Hierarchical Porous Oâ€Doped g <sub>3</sub> N <sub>4</sub> with Enhanced Photocatalytic CO <sub>2</sub> Reduction Activity. Small, 2017, 13, 1603938.	5.2	1,025
4	A Review of Direct Zâ $\in$ Scheme Photocatalysts. Small Methods, 2017, 1, 1700080.	4.6	955
5	In Situ Irradiated Xâ€Ray Photoelectron Spectroscopy Investigation on a Direct Zâ€Scheme TiO <sub>2</sub> /CdS Composite Film Photocatalyst. Advanced Materials, 2019, 31, e1802981.	11.1	714
6	Ag2CrO4/g-C3N4/graphene oxide ternary nanocomposite Z-scheme photocatalyst with enhanced CO2 reduction activity. Applied Catalysis B: Environmental, 2018, 231, 368-380.	10.8	469
7	First principle investigation of halogen-doped monolayer g-C3N4 photocatalyst. Applied Catalysis B: Environmental, 2017, 207, 27-34.	10.8	422
8	Superb adsorption capacity of hierarchical calcined Ni/Mg/Al layered double hydroxides for Congo red and Cr(VI) ions. Journal of Hazardous Materials, 2017, 321, 801-811.	6.5	417
9	Constructing 2D/2D Fe <sub>2</sub> O <sub>3</sub> /g <sub>3</sub> N <sub>4</sub> Direct Z cheme Photocatalysts with Enhanced H <sub>2</sub> Generation Performance. Solar Rrl, 2018, 2, 1800006.	3.1	403
10	The effect of manganese vacancy in birnessite-type MnO2 on room-temperature oxidation of formaldehyde in air. Applied Catalysis B: Environmental, 2017, 204, 147-155.	10.8	362
11	Hollow CoS <sub><i>x</i></sub> Polyhedrons Act as High-Efficiency Cocatalyst for Enhancing the Photocatalytic Hydrogen Generation of g-C <sub>3</sub> N <sub>4</sub> . ACS Sustainable Chemistry and Engineering, 2018, 6, 2767-2779.	3.2	343
12	Room-Temperature Oxidation of Formaldehyde by Layered Manganese Oxide: Effect of Water. Environmental Science & Technology, 2015, 49, 12372-12379.	4.6	297
13	Synthesis of hierarchical porous zinc oxide (ZnO) microspheres with highly efficient adsorption of Congo red. Journal of Colloid and Interface Science, 2017, 490, 242-251.	5.0	266
14	In situ hydrothermal synthesis of g-C 3 N 4 /TiO 2 heterojunction photocatalysts with high specific surface area for Rhodamine B degradation. Applied Surface Science, 2017, 411, 400-410.	3.1	254
15	Hybrid carbon@TiO <sub>2</sub> hollow spheres with enhanced photocatalytic CO <sub>2</sub> reduction activity. Journal of Materials Chemistry A, 2017, 5, 5020-5029.	5.2	240
16	Room-temperature in situ fabrication of Bi 2 O 3 /g-C 3 N 4 direct Z-scheme photocatalyst with enhanced photocatalytic activity. Applied Surface Science, 2018, 430, 273-282.	3.1	216
17	Direct evidence and enhancement of surface plasmon resonance effect on Ag-loaded TiO2 nanotube arrays for photocatalytic CO2 reduction. Applied Surface Science, 2018, 434, 423-432.	3.1	199
18	Review on noble metal-based catalysts for formaldehyde oxidation at room temperature. Applied Surface Science, 2019, 475, 237-255.	3.1	196

#	Article	IF	CITATIONS
19	Synthesis of core-shell TiO 2 @g-C 3 N 4 hollow microspheres for efficient photocatalytic degradation of rhodamine B under visible light. Applied Surface Science, 2018, 430, 263-272.	3.1	193
20	Mechanistic insight into the enhanced photocatalytic activity of single-atom Pt, Pd or Au-embedded g-C 3 N 4. Applied Surface Science, 2018, 433, 1175-1183.	3.1	188
21	Hierarchical porous C/MnO <sub>2</sub> composite hollow microspheres with enhanced supercapacitor performance. Journal of Materials Chemistry A, 2017, 5, 8635-8643.	5.2	174
22	Hierarchical NiS/N-doped carbon composite hollow spheres with excellent supercapacitor performance. Journal of Materials Chemistry A, 2017, 5, 21257-21265.	5.2	174
23	Review on design and evaluation of environmental photocatalysts. Frontiers of Environmental Science and Engineering, 2018, 12, 1.	3.3	170
24	Surface and interface engineering of hierarchical photocatalysts. Applied Surface Science, 2019, 471, 43-87.	3.1	170
25	Formaldehyde and volatile organic compound (VOC) emissions from particleboard: Identification of odorous compounds and effects of heat treatment. Building and Environment, 2017, 117, 118-126.	3.0	169
26	Hierarchical flower-like nickel(II) oxide microspheres with high adsorption capacity of Congo red in water. Journal of Colloid and Interface Science, 2017, 504, 688-696.	5.0	167
27	Hierarchical flower-like C/NiO composite hollow microspheres and its excellent supercapacitor performance. Journal of Power Sources, 2017, 359, 371-378.	4.0	154
28	Adsorptive removal of an anionic dye Congo red by flower-like hierarchical magnesium oxide (MgO)-graphene oxide composite microspheres. Applied Surface Science, 2018, 435, 1136-1142.	3.1	151
29	Hierarchical honeycomb-like Pt/NiFe-LDH/rGO nanocomposite with excellent formaldehyde decomposition activity. Chemical Engineering Journal, 2019, 365, 378-388.	6.6	151
30	ZnO hierarchical microsphere for enhanced photocatalytic activity. Journal of Alloys and Compounds, 2018, 741, 622-632.	2.8	145
31	Few-Layered Graphene-like Boron Nitride: A Highly Efficient Adsorbent for Indoor Formaldehyde Removal. Environmental Science and Technology Letters, 2017, 4, 20-25.	3.9	136
32	Silver Nanoparticle Behavior, Uptake, and Toxicity in <i>Caenorhabditis elegans</i> : Effects of Natural Organic Matter. Environmental Science & Technology, 2014, 48, 3486-3495.	4.6	135
33	Fabrication of flower-like direct Z-scheme β-Bi2O3/g-C3N4 photocatalyst with enhanced visible light photoactivity for Rhodamine B degradation. Applied Surface Science, 2018, 436, 162-171.	3.1	134
34	Enhanced visible-light photocatalytic H <sub>2</sub> -generation activity of carbon/g-C <sub>3</sub> N <sub>4</sub> nanocomposites prepared by two-step thermal treatment. Dalton Transactions, 2017, 46, 10611-10619.	1.6	128
35	Hierarchical C/NiO-ZnO nanocomposite fibers with enhanced adsorption capacity for Congo red. Journal of Colloid and Interface Science, 2019, 537, 736-745.	5.0	123
36	Co 3 O 4 nanorod-supported Pt with enhanced performance for catalytic HCHO oxidation at room temperature. Applied Surface Science, 2017, 404, 426-434.	3.1	110

#	Article	IF	CITATIONS
37	Effects of Natural Organic Matter Properties on the Dissolution Kinetics of Zinc Oxide Nanoparticles. Environmental Science & Technology, 2015, 49, 11476-11484.	4.6	100
38	Fabrication of hierarchical porous ZnO-Al 2 O 3 microspheres with enhanced adsorption performance. Applied Surface Science, 2017, 426, 360-368.	3.1	89
39	Flexible nickel foam decorated with Pt/NiO nanoflakes with oxygen vacancies for enhanced catalytic formaldehyde oxidation at room temperature. Environmental Science: Nano, 2017, 4, 2215-2224.	2.2	87
40	Ultrathin Bi2WO6 nanosheet decorated with Pt nanoparticles for efficient formaldehyde removal at room temperature. Applied Surface Science, 2018, 441, 429-437.	3.1	84
41	Pt/C@MnO2 composite hierarchical hollow microspheres for catalytic formaldehyde decomposition at room temperature. Applied Surface Science, 2019, 466, 301-308.	3.1	81
42	Effect of calcination temperature on formaldehyde oxidation performance of Pt/TiO 2 nanofiber composite at room temperature. Applied Surface Science, 2017, 426, 333-341.	3.1	80
43	The effects of Mn loading on the structure and ozone decomposition activity of MnOx supported on activated carbon. Chinese Journal of Catalysis, 2014, 35, 335-341.	6.9	77
44	Construction of Z-scheme Ag2CO3/N-doped graphene photocatalysts with enhanced visible-light photocatalytic activity by tuning the nitrogen species. Applied Surface Science, 2017, 396, 1368-1374.	3.1	73
45	First-principles investigation of Cu-doped ZnS with enhanced photocatalytic hydrogen production activity. Chemical Physics Letters, 2017, 668, 1-6.	1.2	71
46	Hierarchical Pt/MnO <sub>2</sub> –Ni(OH) <sub>2</sub> Hybrid Nanoflakes with Enhanced Room-Temperature Formaldehyde Oxidation Activity. ACS Sustainable Chemistry and Engineering, 2018, 6, 12481-12488.	3.2	70
47	Fabrication of hierarchical porous ZnO/NiO hollow microspheres for adsorptive removal of Congo red. Applied Surface Science, 2018, 435, 1002-1010.	3.1	67
48	Catalytic decomposition and mechanism of formaldehyde over Pt–Al <sub>2</sub> O <sub>3</sub> molecular sieves at room temperature. Physical Chemistry Chemical Physics, 2017, 19, 6957-6963.	1.3	66
49	Chestnut husk-like nickel cobaltite hollow microspheres for the adsorption of Congo red. Journal of Alloys and Compounds, 2018, 735, 1041-1051.	2.8	66
50	<i>In situ</i> remediation of subsurface contamination: opportunities and challenges for nanotechnology and advanced materials. Environmental Science: Nano, 2019, 6, 1283-1302.	2.2	65
51	Enhanced room-temperature HCHO decomposition activity of highly-dispersed Pt/Al2O3 hierarchical microspheres with exposed {110} facets. Journal of Industrial and Engineering Chemistry, 2017, 45, 197-205.	2.9	63
52	Effects of hierarchical structure on the performance of tin oxide-supported platinum catalyst for room-temperature formaldehyde oxidation. Chinese Journal of Catalysis, 2017, 38, 199-206.	6.9	57
53	Environmental transformation of natural and engineered carbon nanoparticles and implications for the fate of organic contaminants. Environmental Science: Nano, 2018, 5, 2500-2518.	2.2	54
54	Intracellular trafficking pathways in silver nanoparticle uptake and toxicity in <i>Caenorhabditis elegans</i> . Nanotoxicology, 2016, 10, 831-835.	1.6	48

#	Article	IF	CITATIONS
55	Enhanced Hydrolysis of <i>p</i> -Nitrophenyl Phosphate by Iron (Hydr)oxide Nanoparticles: Roles of Exposed Facets. Environmental Science & Technology, 2020, 54, 8658-8667.	4.6	42
56	Direct in situ measurement of dissolved zinc in the presence of zinc oxide nanoparticles using anodic stripping voltammetry. Environmental Sciences: Processes and Impacts, 2014, 16, 2536-2544.	1.7	40
57	Hierarchical NiMn <sub>2</sub> O <sub>4</sub> /rGO composite nanosheets decorated with Pt for low-temperature formaldehyde oxidation. Environmental Science: Nano, 2020, 7, 198-209.	2.2	40
58	Pollution level and seasonal variations of carbonyl compounds, aromatic hydrocarbons and TVOC in a furniture mall in Beijing, China. Building and Environment, 2013, 69, 227-232.	3.0	37
59	Relative Contributions of Copper Oxide Nanoparticles and Dissolved Copper to Cu Uptake Kinetics of Gulf Killifish ( <i>Fundulus grandis</i> ) Embryos. Environmental Science & amp; Technology, 2017, 51, 1395-1404.	4.6	37
60	Synergy between Platinum and Gold Nanoparticles in Oxygen Activation for Enhanced Roomâ€īemperature Formaldehyde Oxidation. Advanced Functional Materials, 2022, 32, .	7.8	37
61	Facile Synthesis of Activated Carbon-Supported Porous Manganese Oxide via in situ Reduction of Permanganate for Ozone Decomposition. Ozone: Science and Engineering, 2013, 35, 308-315.	1.4	35
62	Influence of light wavelength on the photoactivity, physicochemical transformation, and fate of graphene oxide in aqueous media. Environmental Science: Nano, 2018, 5, 2590-2603.	2.2	34
63	Facet-dependent evolution of surface defects in anatase TiO <sub>2</sub> by thermal treatment: implications for environmental applications of photocatalysis. Environmental Science: Nano, 2019, 6, 1740-1753.	2.2	32
64	Facile synthesis of three-dimensional Mn3O4 hierarchical microstructures for efficient catalytic phenol oxidation with peroxymonosulfate. Applied Surface Science, 2019, 495, 143568.	3.1	27
65	Principle and surface science of photocatalysis. Interface Science and Technology, 2020, 31, 1-38.	1.6	24
66	Photochemical decomposition of 1H,1H,2H,2H-perfluorooctane sulfonate (6:2FTS) induced by ferric ions. Journal of Environmental Sciences, 2017, 51, 120-127.	3.2	22
67	Facet-dependent generation of superoxide radical anions by ZnO nanomaterials under simulated solar light. Environmental Science: Nano, 2018, 5, 2864-2875.	2.2	22
68	A Facile Synthesis of Ternary Nickel Iron Sulfide Nanospheres as Counter Electrode in Dyeâ€ <del>S</del> ensitized Solar Cells. Chemistry - A European Journal, 2018, 24, 19032-19037.	1.7	21
69	Current Methods and Prospects for Analysis and Characterization of Nanomaterials in the Environment. Environmental Science & amp; Technology, 2022, 56, 7426-7447.	4.6	19
70	FcγRIIB receptor-mediated apoptosis in macrophages through interplay of cadmium sulfide nanomaterials and protein corona. Ecotoxicology and Environmental Safety, 2018, 164, 140-148.	2.9	15
71	<i>In Vivo</i> Effects of Silver Nanoparticles on Development, Behavior, and Mitochondrial Function are Altered by Genetic Defects in Mitochondrial Dynamics. Environmental Science & Technology, 2022, 56, 1113-1124.	4.6	14
72	In situ synthesis of ternary nickel iron selenides with high performance applied in dye-sensitized solar cells. Applied Surface Science, 2019, 492, 520-526.	3.1	13

CHUANJIA JIANG

#	Article	IF	CITATIONS
73	Design and fabrication of direct Z-scheme photocatalysts. Interface Science and Technology, 2020, 31, 193-229.	1.6	12
74	Photolysis of graphene oxide in the presence of nitrate: implications for graphene oxide integrity in water and wastewater treatment. Environmental Science: Nano, 2019, 6, 136-145.	2.2	11
75	Indoor carbonyl compounds in an academic building in Beijing, China: concentrations and influencing factors. Frontiers of Environmental Science and Engineering, 2012, 6, 184-194.	3.3	9
76	Key factors controlling colloids–bulk soil distribution of polybrominated diphenyl ethers (PBDEs) at an e-waste recycling site: Implications for PBDE mobility in subsurface environment. Science of the Total Environment, 2022, 819, 153080.	3.9	9
77	Sulfide and ferrous iron preferentially target specific surface O-functional groups of graphene oxide: implications for accumulation of contaminants. Environmental Science: Nano, 2020, 7, 462-471.	2.2	7
78	Nanostructured manganese oxides exhibit facet-dependent oxidation capabilities. Environmental Science: Nano, 2020, 7, 3840-3848.	2.2	7
79	Substoichiometric titanium oxide Ti2O3 exhibits greater efficiency in enhancing hydrolysis of 1,1,2,2-tetrachloroethane than TiO2 nanomaterials. Science of the Total Environment, 2021, 774, 145705.	3.9	6
80	Enhanced hydrolysis of 1,1,2,2-tetrachloroethane by multi-walled carbon nanotube/TiO2 nanocomposites: The synergistic effect. Environmental Pollution, 2019, 255, 113211.	3.7	3